

Leveraging of the IUPAC Names and Machine Learning for Assisting Drug Discovery and Development, demonstrated on the Case of Human Tyrosyl-DNA Phosphodiesterase 1 (TDP1) Inhibitors

Mariya L. Ivanova^{1,*}, [ID](#), Nicola Russo¹, [ID](#), Gueorgui Mihaylov², [ID](#) and Konstantin Nikolic¹, [ID](#)

Author affiliations: ¹School of Computing and Engineering, University of West London, London, UK

²Haleon, London, UK

*Corresponding author mariya.ivanova@uwl.ac.uk

Abstract

To assist drug developers, this paper presents three computational approaches demonstrated by a PubChem bioassay focused on human tyrosyl-DNA phosphodiesterase 1 (TDP1) inhibition. First, a machine learning (ML) model based on the RandomForestClassifier (RFC) algorithm was developed that predicted whether a compound was a TDP1 inhibitor with 70.9% accuracy, 73.1% precision, 66.1% recall, 69.4% F1, and 70.8% ROC. It was trained on 94,712 samples and tested on 28,200. The second approach involved reordering the feature importance list following the relative proportion of active cases, providing insights into the expected effect of certain functional groups/fragments on TDP1 inhibition. The third approach was to identify the most and least desirable functional groups/fragments with respect to TDP1 inhibition. The dataset used for these three approaches was obtained by splitting the IUPAC name's samples from the bioassay into basic functional groups/fragments. These tokens were then used to name the features (columns) of the dataset that will be used for the mentioned computational approaches. The values in these columns corresponded to the presence (marked with 1) or absence (marked with 0) of this functional group fragment in the relevant sample. Thus, the dataset used in the study has 5,015 columns (features). The labels of this dataset derived from the initial dataset focused on TDP1 inhibition. In addition to the basic study, the CID_SID ML model was developed, which, using only the compound and substance identifier (CID and SID) data from PubChem, could predict with an accuracy of 85.2%, a precision of 94.2%, a precision of 75%, an F1 of 83.5%, and an ROC of 85.2%.

Introduction

The intention of the work presented here is to develop computational approaches that could contribute to the prediction of the side effects of drugs in the development or give insights for drug discoveries. The need for computational tools was motivated by the report [1], which highlighted that nine out of ten drug candidates that had been entered into trials were never submitted to FDA approval, and that the development of a new drug required around 12 years and over a billion US dollars [2]. So, to develop the proposed supportive computational approaches, ways were sought to leverage the enormous amount of experimental data that has been accumulated at the PubChem repository, along with some relatively simple nomenclature used for naming the compounds and substances. Here, an investigation was made into how the information encoded in the names of compounds, generated according to the International Union of Pure and Applied Chemistry (IUPAC) [3] nomenclature, could be utilized. These unique IUPAC names are based on the chemical composition and structures of the compounds and enable clear communication amongst chemists worldwide.

IUPAC names have been previously used by iupacGPT [4] and BioT5+ [5] for computational biochemistry for drug discoveries. While both are large language models (LLM), there are significant differences between them. The iupacGPT approach is centralized around IUPAC names treating them like a chemist's natural language to design new compounds and predict their functionalities. BioT5+ thought used IUPAC names like a feature in broadened data which integrates literature from PubMed and bioRxiv, molecular data like SELFIES from PubChem, protein sequences from UniRef50 and learning simultaneously across 15 different tasks and 21 benchmark datasets [5]. However, both, as LLMs are not exempt of "hallucination" which in chemical domain means fabrication of non-existent facts, such as incorrect properties, non-existing interactions, fictitious reactions; invalid SMILES/SELFIES/IUPAC names or invalid protein sequences. [6] Prediction of IUPAC names based on the International Chemical Identifier (InChI) of the chemicals has been conducted by implementing tokenization of the names character by character. This ML achieved 91% of accuracy for the organic molecules with an exemption of macrocycles [7] giving insights for vice-versa implementation of the approach utilized data encoded in IUPAC. Another insightful study [8] that includes IUPAC names demonstrates the generation of these names based on atomic force microscopy (AFM) images performed by deep learning (DL). Overall, extensive research of the publicly available literature revealed that up to date the approach presented in the current paper has not been reported. It incorporates two methodologies that used data derived from IUPAC names to generate lists with functional groups that could facilitate the researchers in drug development based on their human intelligence.

To demonstrate the proposed methodologies, the PubChem AID 686978 bioassay, focused on the human tyrosyl-DNA phosphodiesterase 1 (TDP1) was used [9]. This bioassay aims to identify active inhibitors of TDP1, with the idea of adding to TDP1-mediated repair pathway for cancer treatment. Although TDP1 is not an essential protein, it turned out to be crucial for cell survival under specific conditions, such as cancer treatment with topoisomerase I toxin (camptothecin: CPT). For more details about the bioassay protocol, please refer to the documentation [9]. The choice of TDP1 as the object used for demonstration of the current study's approach was driven by enzyme's importance such as its ability to repair damaged DNA caused by topoisomerase 1 cleavage complexes [10]. This TDP1 ability has application in cancer treatment and has been clinically tested on 150 patients with non-small-cell lung cancer [11]. To find out how TDP1 repair the DNA-protein crosslinks (DPC), damaged DNA lesions that lead to genomic instability and cell death, a study has been conducted and demonstrate the endogenous nature of TDP1 to repair DPCs [12, 13]. There are also non-cancer related roles of TDP1, its mutation causes spinocerebellar ataxia with axonal neuropathy 1 (SCAN1) [14, 15]. This is a rare neurodegenerative disorder for which no cure has yet been found [16, 17].

The dataset of the above-mentioned bioassay PubChem AID 686978 contained 424,883 samples described by 48 features [9]. Of these samples, 64,192 were classified as active, 116,652 as inconclusive, and 243,131 as inactive. The IUPAC names of the considered compounds needed for the study were retrieved from the PubChem database and merged with the labels of the bioassay. In order for the inactive compounds in the mentioned bioassay to be reduced, a second bioassay was involved, PubChem AID 1996 on Aqueous Solubility from Molecular Libraries Small Molecule Repository Stock Solutions, which bioassay was used like a filter to reduce the inactive compound because only the compounds common for both bioassays were kept [18]. The PubChem AID 1996 bioassay contained 57,859 rows of

samples, 40,860 of which were labeled as soluble and 17,573 like insoluble small biomolecules, which samples were described by 30 columns of features. Although this bioassay was focused on water solubility, solubility by itself was not considered in the presented research. For the purpose of the study only the column with CIDs was used to reduce the inactive compounds in the PubChem AID 686978 bioassay.

The available literature was explored, and observed variety of AI approaches assisted in drug discovery [19]; generation of attributes for ML based on atomic features [20]; comparing the results of ten ML algorithms to predict the age of intervention that would improve the efficacy of the treatment of spinocerebellar ataxia type 3 [21]; ML predictions based on ¹³C NMR spectroscopic data derived from simplified molecular input line entry system (SMILES) [22]; using SMILES notations transformed by the RDKit cheminformatics toolkit into numerical data that has been used for developing of a ML model to predict potential TDP1 inhibitors [23]. However, to date, the methodology presented in this article has not been reported.

A CID_SID machine learning model was developed as a supplementary tool, enabling drug researchers, using only the sample PubChem CID and SID, computationally to screen compounds for TDP1 inhibition that primarily have been designed for other purposes [24]. The identifiers of samples, by nature, do not contain data usable for ML training and testing. However, PubChem generates their Identifiers using an algorithm that considers the structure and similarity among the compounds and substances. A study used this fact and developed CID_SID ML models, predicting D3 dopamine receptor antagonists, Rab9 promoter activators, DNA damage-inducible transcript 3 inhibitors and M1 muscarinic receptor antagonists [24]. The approach was explored later by another study to predict dopamine D1 receptor antagonists, confirming the applicability of such methodology for different case studies [22]. So, such a CID_SID ML model was developed to predict TDP1 inhibitors.

Methodology

The first methodology developed a ML model that can predict a considered functionality and extract the feature importance. The second methodology generates hierarchical order of functional groups based on their presence in the composition of the considered small biomolecules explored for the functionality of interest. ML performed during the study utilized the interpretation of the RFC [25] by the scikit learn library for ML [26] and compiled to the best relevant practice recommended in the literature [27] for data preprocessing, training, predicting, and evaluating the results with the relevant ML metrics.

The methodology is illustrated in Figure1. To rectify the significant class imbalance within the initial bioassay a refined dataset was obtained by identifying and retaining only compounds common to both the original dataset and PubChem AID 1996 [18]. The reduced inactive compounds were then concatenated with the active compound from the original PubChem AID 686978 [9]. The PubChem CIDs, SIDs, and the relevant labels were extracted from the resulting dataset. A list of CID values was then created and used to download the IUPAC names from the PubChem database.

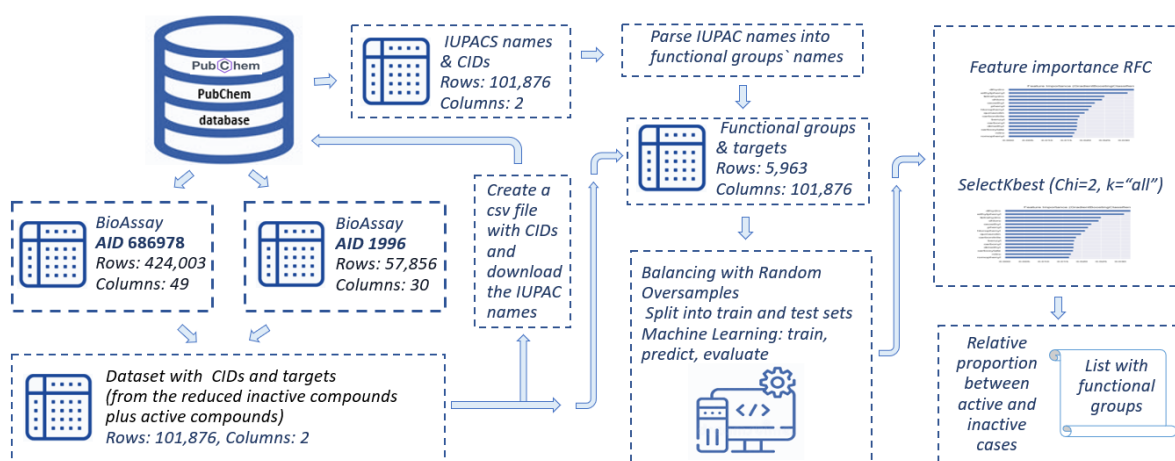


Figure 1. Methodology of the ML model utilizing IUPAC names, PubChem bioassay data and the scikit learn ML library

Once the IUPAC names of the considered compounds were downloaded, they were parsed, leaving only the strings with four or more letters, Table 1. This parsing aimed at identifying the functional groups and fragments that indicate specific parts of a larger molecule. These strings were used to create columns in the data frame. The presence of a given functional group in a sample was marked with digit 1, and the absence with digit 0. Thus, the newly formed data frame contained information for the presence or absence of a particular functional group in the IUPAC name of the considered compounds. The resulting data frame was merged with the data frame containing the labels based on the commonality for both data frame CIDs.

The combined data frame was used for ML with the Scikit Learn software implementation of the Random Forest Classifier (RFC) algorithm [25, 26]. For this purpose, the dataset was split into test and train sets, assuring an equal number of samples for each class in the test sets. The final balancing of the training data was performed by the Random OverSampler, whose strategy randomly repeated samples from the minority class until a balance training dataset was obtained. The training and testing sets were then used for training, predicting and evaluating the ML model based on the RFC strategy. Five-fold cross-validation was performed to estimate how well the RFC will perform on unseen data. The principal component analysis (PCA) was applied to explore whether this statistical technique, which provides dimensionality reduction, would improve the performance of the ML model. Hyperparameter tuning was executed by the open-source framework Optuna [28], designed to automate this process. Given that the data generation accumulates a high number of columns/ features, it was essential that the PubChem bioassay must contain a significant number of samples, especially those labelled as Active compounds, such as the chosen for the demonstration purpose PubChem AID 686978 [9].

Table 1. Methodology. Parsing/breaking down the IUPAC names into tokens/strings equal or longer than four letters and using these tokens/strings to create the data frame features. Counting the presence of the functional groups in the compound's content with 1 for presence and 0 for absence of the relevant feature group/fraction in the content of the small biomolecule.

composition of the inactive small biomolecules and did not participate in the composition of any active biomolecule.

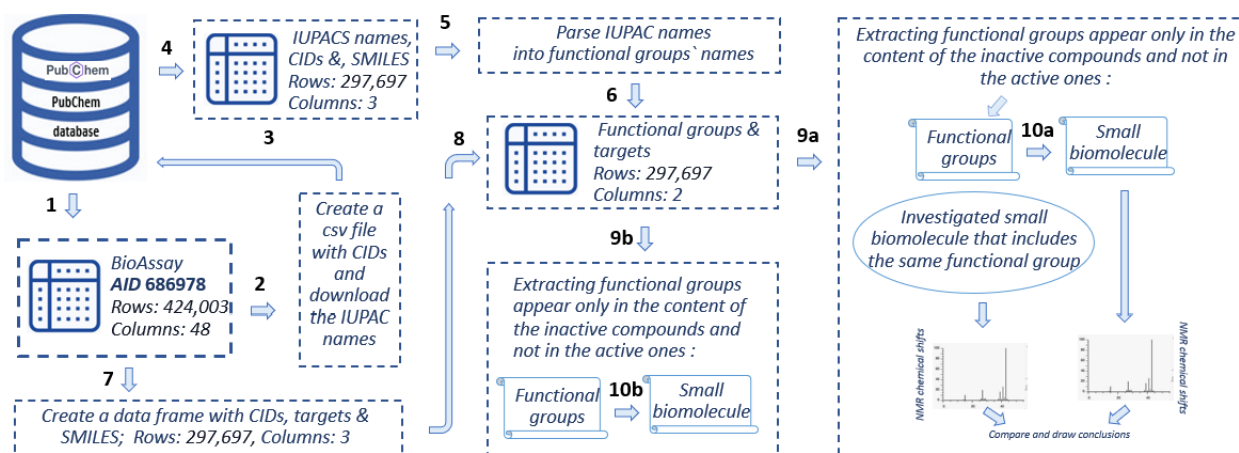


Figure 2. Methodology generating ranking of the functional groups according to their presence in the biomolecule content

In addition to the main study, following the methodology used for building the CID_SID ML model [26], one for TDP1 was developed. For this purpose, CIDs, SIDs and the labels were extracted from the PubChem AID 686978 [9]; the data imbalance was handled initially by filtering with the PubChem AID 1996 [18] bioassay and finished by the balance oversampling, explained above; ML was performed with the classifiers Decision Tree (DTC), Random Forest (RFC), Gradient Boosting (GBC), XGBoost (XGBC) and Support Vector (SVC), whose metrics were compared and picked up the most suitable for the particular CID_SID ML model case study. A rigorous evaluation process was conducted in order for the model's predictive capability to be maximized, such as five-fold cross-validation, hyperparameter optimization, and overfitting analysis.

Results and Discussion

Predictive Power of the Algorithm

Removing the isomers without keeping any sample of them reduced the active compounds to 61,471, inconclusive to 112,867 and inactive to 236,226. After this dataset reduction and filtered it with the PubChem AID 1996 [18] bioassay dataset, 40,404 inactive compounds remained. Concatenating these reduced inactive compounds with the active compounds (without the isomers) yielded the final dataset of 101,860 samples. Downloading the IUPAC names of these samples from the PubChem database and parsing these names into strings with four or more letters, in the way explained in section Methodology, resulted in the generation of 5,963 columns.

The ML model, based on Random Forest Classifier algorithm was trained by 64,625 samples and tested by 28,200 samples and obtained initially accuracy 79.3%, precision 79.7, recall 78.5, F1 79.1%, ROC 79.3%. The five-fold cross-validation results are presented in Table 2, where the mean accuracy across the five folds is close to the single accuracy of the ML model.

Table 2. Five-fold cross-validation of RFC with StratifiedKFold

| Metrics | Fold | | | | | Average across the folds | |
|------------------|-------|-------|-------|-------|-------|--------------------------|--------------|
| | 1 | 2 | 3 | 4 | 5 | | |
| Accuracy [%] | 78.47 | 78.12 | 78.95 | 77.94 | 78.60 | 78.42±0.36 | |
| Precision [%] | 87.24 | 86.87 | 87.82 | 87.05 | 87.30 | 87.12±0.15 | |
| Recall [%] | 77.90 | 77.71 | 78.91 | 77.16 | 78.07 | 77.95±0.57 | |
| F1-Score [%] | 82.31 | 82.04 | 82.82 | 81.81 | 82.42 | 82.28±0.34 | |
| ROC AUC [%] | 86.72 | 86.14 | 86.95 | 86.24 | 86.94 | 86.60%±0.34 | |
| Confusion Matrix | TN | 4182 | 4149 | 4174 | 4174 | 4184 | 4172.6±12.48 |
| | FP | 1079 | 1112 | 1104 | 1087 | 1076 | 1091.6±14.09 |
| | FN | 2093 | 2111 | 1997 | 2163 | 2077 | 2088.2±54.00 |
| | TP | 7378 | 7360 | 7474 | 7308 | 7395 | 7387.4±54.04 |

However, scrutinizing for overfitting revealed that after the maximum depth of the trees (max_depth) was equal to 23 the deviation between the train and test accuracy became higher than 5% which was accepted as an indication for overfitting. At this point, the train accuracy was 74.8% and the test accuracy 70.2%. Scrutinizing for overfitting is illustrated in Figure 3.



Figure 3. Overfitting analysis of the IUPAC RFC ML model: prediction accuracy vs maximum depth of the decision tree. The blue line is the training accuracy. The orange line is the test accuracy. The deviation between the testing and training accuracy higher than 5% was considered as an indication of overfitting.

So, given this observation, the RFC was performed with **max_depth=23** and achieved:

- (i) Accuracy (correct predictions out of all predictions): 70.5%.
- (ii) Precision (all true positive predictions out of all positive predictions): 73,4%.
- (iii) Recall/Sensitivity (all true positive predictions out of all actual positive cases): 64.2%.
- (iv) F1-score, i.e. the harmonic mean of precision and recall: 68.5%.
- (v) ROC (Receiver Operating Characteristic, true positive rate against false positive rate): 70.5%

Dimensionality Reduction

The implementation of PCA reduced the number of features from 5, 963 to 44. However, the ML model performed with the PCA reduction of the features obtained accuracy 69.7%,

precision 65.8%, recall 82.1, F1 73%, ROC 69.7% which metrics values were a bit lower compared to these obtained by the ML model without PCA reduction of the features.

Final ML model based on PubChem and IUPAC data and RFC

Hyperparameter tuning was performed by Optuna. However, the best parameters suggested by Optuna, i.e., `n_estimators=191`, `max_depth=12`, `min_samples_split=5`, `min_samples_leaf=2`, `max_features='log2'`, `criterion='gini'`, which were the result of five study trials, achieved accuracy of 70.33 which didn't improve the performance of the ML model. Thus, the final ML model remained with the default hyperparameter values. To visualize the results, the confusion matrix of the final IUPAC RFC ML model is provided in Figure 5 and the classification report in Table 4.

Table 4 Classification report of the IUPAC RFC ML model

| | precision | recall | F1-score | support |
|---------------------|-----------|--------|----------|---------|
| Active (target 1) | 0.69 | 0.77 | 0.73 | 14100 |
| Inactive (target 0) | 0.74 | 0.65 | 0.69 | 14100 |
| accuracy | | | 0.71 | 28200 |
| macro avg | 0.71 | 0.71 | 0.71 | 28200 |
| Weighted avg | 0.71 | 0.71 | 0.71 | 28200 |

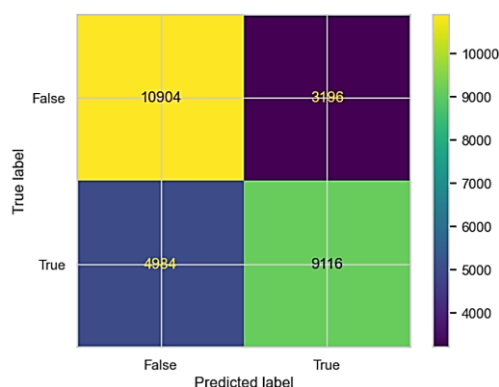


Figure 5. The IUPAC RFC ML model confusion matrix.

Identification of the relevant functional groups for the inhibitory action

The feature importance analysis indicates which functional groups could be the most relevant for a specific chemical interaction. In Figure 3 below, a list of 24 functional groups with the highest relevance in respect to the inhibition of TDP1 is shown. It should be noted that the computations were based on the mutual influence between all features. Here, the first 24 functional groups out of the list of 5,963 groups are shown.

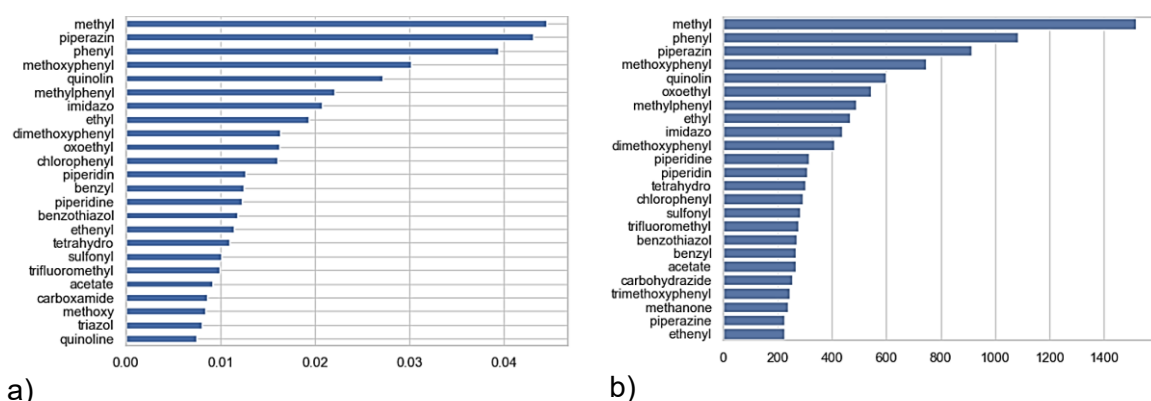


Figure 4. Feature (functional group) importance ranking for the prediction of TDP1 inhibitors.
 a) Scikit Learn Feature Importance algorithm for the Random Forest Classifier. b) Chi2 algorithm.

However, feature importance in a binary classifier tells how much each feature contributes to the model's overall predictive power, but it does not directly indicate whether a feature is characteristic of the active or inactive class. In other words, the machine learning feature importance algorithms give us all functional groups that are correlated with the inhibition of a specific substance, but it does not necessarily mean that they are actively contributing to the effect. Some of these functional groups could appear in the compounds which are not inhibitors. Therefore, in order to prioritize those functional groups with a higher chance of being real inhibitors, the ratio (or relative proportion) of the active and inactive compounds containing that functional group was calculated. The resulting combined importance ranking list was reordered based on this metric and shown in Table 3. Notably *imidazo* was identified to be with highest relative proportion of the active cases of 8.33, followed by *ethenyl* with 6.95 and *trimethoxyphenyl* with 6.14. On the bottom of this feature list was *carbohydrazide* with 0.27 relative proportion of the active cases.

Table 3. Relevance of functional groups regarding the prediction of TDP1 inhibitors, by using the Feature Importance algorithm (column 1), and reordered (in col. 2) on the basis of the value for the ratio of the number of Active inhibitor substances (col. 4) and Inactive (col.5), which is give in col.6.

| Position according to Feature Importance algorithm | Position according to relative proportion of the active cases | Functional group/fragment | Number of substances that are active inhibitors and contain this group (Active cases) | Number of substances that are not active inhibitors and contain this group (Inactive cases) | Percentage of Active cases | Ratio of Active and Inactive cases for the functional group |
|--|---|---------------------------|---|---|----------------------------|---|
| 9 | 1 | <i>imidazo</i> | 1050 | 126 | 89% | 8.33 |
| 21 | 2 | <i>ethenyl</i> | 591 | 85 | 87% | 6.95 |
| 20 | 3 | <i>trimethoxyphenyl</i> | 731 | 119 | 86% | 6.14 |
| 6 | 4 | <i>quinolin</i> | 1785 | 299 | 86% | 5.97 |
| 3 | 5 | <i>piperazin(e)*</i> | 4211 | 870 | 83% | 4.84 |
| 24 | 6 | <i>tetrahydro</i> | 1259 | 302 | 81% | 4.17 |
| 15 | 7 | <i>benzothiazol</i> | 1375 | 368 | 79% | 3.74 |
| 12 | 8 | <i>sulfonyl</i> | 1512 | 427 | 78% | 3.54 |
| 13 | 9 | <i>piperidine</i> | 1839 | 547 | 77% | 3.36 |

| | | | | | | |
|----|-----------|------------------------|-------|------|-----|-------------|
| 10 | 10 | <i>dimethoxyphenyl</i> | 2647 | 806 | 77% | 3.28 |
| 25 | 11 | <i>methanone</i> | 1831 | 596 | 75% | 3.07 |
| 2 | 12 | <i>phenyl</i> | 8524 | 2941 | 74% | 2.90 |
| 19 | 13 | <i>piperidin</i> | 2457 | 851 | 74% | 2.89 |
| 17 | 14 | <i>trifluoromethyl</i> | 2406 | 865 | 74% | 2.78 |
| 14 | 15 | <i>benzyl</i> | 2458 | 892 | 73% | 2.76 |
| 4 | 16 | <i>methoxyphenyl</i> | 6966 | 2559 | 73% | 2.72 |
| 8 | 17 | <i>methylphenyl</i> | 5961 | 2383 | 71% | 2.50 |
| 11 | 18 | <i>chlorophenyl</i> | 4749 | 2004 | 70% | 2.37 |
| 7 | 19 | <i>ethyl</i> | 8252 | 3752 | 69% | 2.20 |
| 1 | 20 | <i>methyl</i> | 20205 | 9283 | 69% | 2.18 |
| 16 | 21 | <i>carboxamide</i> | 9495 | 4910 | 66% | 1.93 |
| 5 | 22 | <i>oxoethyl</i> | 2420 | 3059 | 44% | 0.79 |
| 22 | 23 | <i>acetate</i> | 655 | 982 | 40% | 0.67 |
| 18 | 24 | <i>carbohydrazide</i> | 126 | 460 | 22% | 0.27 |

Since the IUPAC names were broken down and the results used directly, the appearance of a functional group or fragment with different spellings should be handled appropriately by calculating its mean value, such as '*piperazin*' and '*piperazine*' in Table 2. In that case, they should be collated. For example, '*piperazin*' and '*piperazine*' have the relative proportion values of 5.06 and 4.29, respectively. So, the relative proportion of the active and inactive cases for '*piperazine*' is calculated to be 4.68.

There are other ways of ranking the functional groups. For example, the ranking can be based on their participation in only one type of the cases (active or inactive):

- (i) For the functional groups that participate only in active (i.e. it is a TDP1 inhibitor) small biomolecule content and in no inactive compounds, the leading functional group was oxonaphthalen with 25 active cases followed by *methylsulfonylpyrimidine* with 22 and *tetrahydroindol* with 20 active cases. The entire ranking list of 2,178 functional groups participated in the content of the active small biomolecule is available on GitHub [29].
- (ii) For the functional groups that participate only in inactive (i.e. it is not a TDP1 inhibitor) small biomolecule composition and in none of active on the top on this list was *ylbutanediamide* with 104 inactive cases followed by *oxopiperazin* with 100 and *tetrazabicyclo* with 99. The entire ranking list of 6,243 functional groups participated only in the content of the inactive small biomolecule is available on GitHub [30].

Furthermore, given the correlation between the chemical shifts of a biomolecule provided by the ¹³C NMR spectroscopy and its functionality [31, 32], it was hypothesised that when a tested compound contains one of the extracted functional groups/fragments and its ¹³C NMR spectroscopy data resembles of the ¹³C NMR spectroscopy data of the source compound of this functional group/fragments, there is a high probability that the tested compound is a TDP1 inhibitor. One of the tools that can provide such a comparison of the NMR spectroscopy data is the ACD/Labs [33].

Addition model for TDP1 inhibitors classification: CID_SID ML model

The CID_SID ML model that was developed beyond the main study to aid drug discovery researchers interested in TDP1 inhibition, achieved accuracy 86%, precision 93.3%, recall

77.5%, F1 84.7%, ROC 86% with XGBC, followed by GBC with accuracy 85.1%, precision 94.5%, recall 74.6%, F1 83.4%, ROC 85.1% (Table 5). The five-fold cross validation of the optimal ML model in this case, XGBC, obtained mean accuracy 85.1%, precision 94.5%, recall 74.6%, F1 83.4%, ROC 85.1% Table 6. The results were achieved by training the ML model with 100,942 samples and tested by 22,000 samples.

Table 5. Evaluation metrics for the CID_SID machine learning model

| Algorithm | Accuracy | Precision | Recall | F1-score | ROC |
|---------------|----------|-----------|--------|----------|-------|
| XGBoost | 0.861 | 0.934 | 0.777 | 0.848 | 0.861 |
| GradientBoost | 0.851 | 0.942 | 0.749 | 0.834 | 0.851 |
| RandomForest | 0.846 | 0.855 | 0.835 | 0.845 | 0.846 |
| K-nearest | 0.834 | 0.848 | 0.815 | 0.831 | 0.834 |
| Decision | 0.805 | 0.776 | 0.857 | 0.815 | 0.805 |
| SVM | 0.788 | 0.924 | 0.627 | 0.747 | 0.788 |

Table 6 Five-fold cross-validation results for the CID_SID machine learning models with XGB algorithm

| Metrics | Fold | | | | | Average across the folds | |
|------------------|-------|-------|-------|-------|-------|--------------------------|--------------|
| | 1 | 2 | 3 | 4 | 5 | | |
| Accuracy [%] | 83.78 | 83.91 | 83.92 | 83.66 | 84.74 | 84.00±0.38 | |
| Precision [%] | 90.70 | 90.49 | 90.22 | 90.44 | 91.27 | 90.62±0.36 | |
| Recall [%] | 82.81 | 83.29 | 83.61 | 82.89 | 83.88 | 83.30±0.41 | |
| F1-Score [%] | 86.58 | 86.74 | 86.79 | 86.50 | 87.42 | 86.81±0.32 | |
| ROC AUC [%] | 91.05 | 91.10 | 91.08 | 90.85 | 91.54 | 91.12%±0.23 | |
| Confusion Matrix | TN | 5024 | 4997 | 4966 | 4997 | 5071 | 5011±35.17 |
| | FP | 857 | 884 | 915 | 884 | 810 | 870±35.17 |
| | FN | 1735 | 1687 | 1654 | 1727 | 1627 | 1686±41.44 |
| | TP | 8360 | 8407 | 8440 | 8367 | 8467 | 8408.2±41.21 |

The XGBC model was scrutinized for overfitting, tracing the deviation between test and train accuracy (Figure 6). It was observed that the overfitting started at max_depth= 7, where the test accuracy was 86.1%. So, the XGBC model was rerun with the tuned hyperparameter max_depth=7, and obtained accuracy 86.1%, precision 93.1%, recall 77.9%, F1 84.8%, ROC 86.1%. To visualize the results the confusion matrix of the XGBC is provided in Figure 7 and the classification report in Table 7. The hyperparameter tuning with Optuna obtained 85.6% accuracy, where the hyperparameters were tuned, as follows: max_depth=10, learning_rate=0.0979, n_estimators=381, subsample=0.9643, colsample_bytree=0.6768, gamma= 0.41188, reg_lambda=0.2278899, min_child_weight=6. So, the final CID_SID RFC ML model remained with its default hyperparameters because it performed slightly better than the Optuna hyperparameters tuned ML model.



Figure 6 Scrutinizing for overfitting of the CID_SID XGBC ML model that predicts the TDP1 inhibitors. The blue line is the train accuracy. The orange line is the test accuracy. The deviation between the test and train accuracy higher than 5% is an indication for overfitting.

Table 7 The CID_SID XGBC ML model classification report.

| | precision | recall | F1-score | support |
|---------------------|-----------|--------|----------|---------|
| Active (target 1) | 0.80 | 0.95 | 0.87 | 11000 |
| Inactive (target 0) | 0.94 | 0.77 | 0.85 | 11000 |
| accuracy | | | 0.86 | 22000 |
| macro avg | 0.87 | 0.86 | 0.86 | 22000 |
| Weighted avg | 0.87 | 0.86 | 0.86 | 22000 |

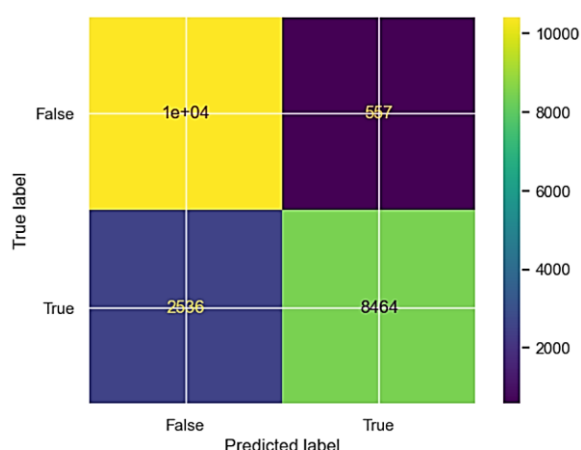


Figure 7. The CID_SID XGBC ML model confusion matrix

Conclusion

The presented approach can be applied to any other case study whose bioassay has a significant number of labelled records. Although the obtained descending ranks with the

functional groups were computationally based, the expectations are that it corresponds to the reality because the computational approach were based on real life data obtained by HTS. Thus, the approach could benefit the early stage of drug discovery, directing the choice for functional groups with higher priority than others. The additionally developed CID_SID ML model was complimentary for the researchers interested in the TDP1 inhibitors, giving them a user-friendly ML model for computational screening of their compound for potential TDP1 inhibitors.

Limitations

- Since the parsing of IUPAC names leads to generation of a few thousand features, the dataset necessary for both the ML models and the list generations require sufficient amount of data. This in turn would meet the recommended thumb up ML rule that the number of rows should be ten times more than the number of columns. Technique such as HTS can provide the needed samples result.
- A comparison of the results obtained by the presented approach and Bio5T+ confirmed in a chemical laboratory would provide clarification regarding the level of credibility and preferences between both.

Scientific contribution

- A methodology for developing an ML model that can predict the considered functionality of a small biomolecule solely relying on its IUPAC name and thus contribute to prediction of such a side effect of already designed compounds.
- An ML model using the IUPAC name of a small biomolecule to predict whether it is a TDP inhibitor. The model can contribute to prediction of such a side effect of already designed compounds.
- A methodology generating a list with functional groups reordered according to the relative proportions of the functional groups participating in the active and inactive cases of the considered bioassay. The list originated from the algorithms which classify the importance of the features in the considered ML model and thus carrying the potential of the pattern used for the ML prediction. It was hypothesized that the relative proportion higher than five gives a reason for expectation that the functional group will contribute for obtaining of the small biomolecule functionality of interest.
- A methodology generating a list with functional groups according to their participating only in the active cases and in no one inactive case. The usage of these functional groups is a prerequisite for obtaining a
- Nominating imidazo based on computational algorithms to carry potential to contribute to TDP1 inhibition. It gives an insight for choice of functional groups drug design.
- Nominating oxonaphthalen based on their participation only in TDP1 inhibitor for having the potential to contribute to TDP1 inhibition when they participate in other small biomolecule composition. It gives an insight into the choice of functional groups during drug design or checking for such a functionality of already designed compound.

Author Contributions

MLI, NR, GM and KN conceptualized the project and designed the methodology. MLI, NR and GM processed the data. MLI and NR wrote the code. KN supervised the project. All authors were involved with the writing of the paper.

Acknowledge

MLI thanks the UWL Vice-Chancellor's Scholarship Scheme for their generous support. We sincerely thank NIH for providing access to their PubChem database. The article is dedicated to Luben Ivanov

Data and Code Availability Statement

The raw data used in the study is available through the PubChem portal:

<https://pubchem.ncbi.nlm.nih.gov/>

The code generated during the research is available on GitHub:

https://github.com/articlesmli/IUPAC_ML_model_TDP1

Conflicts of Interest

The authors declare no conflict of interest

References

- [1] H. Guo, X. Xing, Y. Zhou, W. Jiang, X. Chen, T. Wang, et al. A Survey of Large Language Model for Drug Research and Development. *IEEE Access* **13** (2025) 51110-51129. <https://doi.org/10.1080/14656566.2022.2161366>
- [2] J. M. Metselaar, T. Lammers Challenges in nanomedicine clinical translation. *Drug Deliv. and Transl. Res.* **10** (2020) 721–725 <https://doi.org/10.1007/s13346-020-00740-5>
- [3] International Union of Pure and Applied Chemistry. Home page <https://iupac.org/>
- [4] J. Mao, J. Wang, K-H. Cho, K. T. No (2023) iupacGPT: IUPAC-based large-scale molecular pre-trained model for property prediction and molecule generation. *ChemRxiv*. (2023). <https://doi.org/10.26434/chemrxiv-2023-5kjhv>
- [5] Q. Pei, L. Wu, K. Gao, X. Liang, Y. Fang, J. Zhu, et al. BioT5+: Towards Generalized Biological Understanding with IUPAC Integration and Multi-task Tuning. *ArXiv* (2024) <https://doi.org/10.48550/arXiv.2402.17810>
- [6] S. M. Reed. Augmented and Programmatically Optimized LLM Prompts Reduce Chemical. *Journal of Chemical Information and Modeling* **65** (2025) 4274-4280 <https://doi.org/10.1021/acs.jcim.4c02322>
- [7] J. Handsel, B. Matthews, N.J. Knight, J.C Simon Translating the InChI: adapting neural machine translation to predict IUPAC names from a chemical identifier. *J Cheminform* **13** (2021) 79. <https://doi.org/10.1186/s13321-021-00535-x>
- [8] J. Carracedo-Cosme, C. Romero-Muñiz, P. Pou, R. Pérez. Molecular Identification from AFM Images Using the IUPAC Nomenclature and Attribute Multimodal Recurrent Neural Networks, *ACS Appl. Mater. Interfaces* **15** (2023) 22692–22704. <https://doi.org/10.1021/acsami.3c01550>
- [9] National Institutes of Health, PubChem, qHTS for Inhibitors of Human Tyrosyl-DNA Phosphodiesterase 1 (TDP1): qHTS in Cells in Absence of CPT <https://pubchem.ncbi.nlm.nih.gov/bioassay/686978> (Accessed 10 February 2025)
- [10] H. Zhang, Y. Xiong, D. Su, et al. TDP1-independent pathways in the process and repair of TOP1-induced DNA damage. *Nature Communications* **13**, 4240 (2022). <https://doi.org/10.1038/s41467-022-31801-7>
- [11] A-K. Jakobsen, S. Yuusufi, L. B. Madsen, P. Meldgaard, B. R. Knudsen and M. Stougaard. TDP1 and TOP1 as targets in anticancer treatment of NSCLC: Activity and protein level in normal and tumor tissue from 150 NSCLC patients correlated to clinical data. *Lung Cancer* **164** (2022) 23-32. <https://doi.org/10.1016/j.lungcan.2021.12.010>

- [12] I. Anticevic, C. Otten, L. Vinkovic, L. Jukic and M. Popovic. Tyrosyl-DNA phosphodiesterase 1 (TDP1) and SPRTN protease repair histone 3 and topoisomerase 1 DNA–protein crosslinks in vivo. *Open Biology* **13** (2023)13230113. <http://doi.org/10.1098/rsob.230113>
- [13] C. G. Goh, A. S. Bader, T-A. Tran, R. Belotserkovskaya, G. D’Alessandro and S. P. Jackson. TDP1 splice-site mutation causes HAP1 cell hypersensitivity to topoisomerase I inhibition. *Nucleic Acids Research* (2024) <https://doi.org/10.17863/CAM.113417>
- [14] H. Takashima, C. Boerkoel, J. John *et al.* Mutation of *TDP1*, encoding a topoisomerase I–dependent DNA damage repair enzyme, in spinocerebellar ataxia with axonal neuropathy. *Nature Genetics* **32**, (2022) 267–272. <https://doi.org/10.1038/ng987>
- [15] M. Geraud, A. Cristini, S. Salimbeni, N. Bery, G. Capranico, O. Sordet, et al. TDP1 Mutation Causing SCAN1 Neurodegenerative Syndrome Hampers the Repair of Transcriptional DNA Double-Strand Breaks. *Cell Reports* **43** (2024) 114214. <https://doi.org/10.1016/j.celrep.2024.114214>
- [16] M.A.M. Salih, H. Takashima and C. F. Boerkoel. Spinocerebellar Ataxia with Axonal Neuropathy Type 1. 2007 Oct 22 [Updated 2022 Jun 30]. In: Adam MP, Feldman J, Mirzaa GM, et al., editors. University of Washington, Seattle. Available from: <https://www.ncbi.nlm.nih.gov/books/NBK1105/> (Accessed 10 February 2025)
- [17] P. Scott, A. A. Kindi, A. A. Fahdi, N. A. Yarubi, Z. Bruwer, S. A. Adawi, R. Nandhagopal, Spinocerebellar ataxia with axonal neuropathy type 1 revisited, *Journal of Clinical Neuroscience* **67** (2019) 139-144. <https://doi.org/10.1016/j.jocn.2019.05.060>
- [18] National Institutes of Health, PubChem, Aqueous Solubility from MLSMR Stock Solutions. <https://pubchem.ncbi.nlm.nih.gov/bioassay/1996> (Accessed 10 February 2025)
- [19] I. Mohammed, and S. R. Sagurthi. Current Approaches and Strategies Applied in First-in-class Drug Discovery. *ChemMedChem* (2024) e202400639. <https://doi.org/10.1002/cmdc.202400639>
- [20] M. L. Ivanova, N. Russo, N. Djaid, and K. Nikolic. Application of Machine Learning for Predicting G9a Inhibitors. *Digital Discovery* **3** (2024) 2010-2018. <https://doi.org/10.1039/D4DD00101J>
- [21] D. Ru, J. Li, O. Xie, L. Peng, H. Jiang, and R. Qiu, (2022) Explainable artificial intelligence based on feature optimization for age at onset prediction of spinocerebellar ataxia type 3. *Frontiers in Neuroinformatics* **16** (2022) 978630. <https://doi.org/10.3389/fninf.2022.978630>
- [22] M. L. Ivanova, N. Russo, and K. Nikolic. Leveraging ¹³C NMR Spectroscopic Data Derived from SMILES to Predict the Functionality of Small Biomolecules by Machine Learning: a Case Study on Human Dopamine D1 Receptor Antagonists. *ArXiv*, 2025, <https://doi.org/10.48550/arXiv.2501.14044>

[23] C. H. Lai, A. P. K. Kwok, and K. C. Wong. Cheminformatic Identification of Tyrosyl-DNA Phosphodiesterase 1 (Tdp1) Inhibitors: A Comparative Study of SMILES-Based Supervised Machine Learning Models. *Journal of Personalized Medicine* **14** (2024) 981.
<https://doi.org/10.3390/jpm14090981>

[24] M. L. Ivanova, N. Russo, and K. Nikolic. Predicting Novel Pharmacological Activities of Compounds Using PubChem IDs and Machine Learning (CID-SID ML Model). *ArXiv*, 2025.
<https://doi.org/10.48550/arXiv.2501.02154>

[25] L. Breiman. Random Forests. *Machine Learning* **45** (2001) 5–32.
<https://doi.org/10.1023/A:1010933404324>

[26] F. Pedregosa, G. Varoquaux, A. Gramfort, V. Michel, B. Thirion, O. Grisel *et al.* Scikit-learn: Machine Learning in Python. *Journal of Machine Learning Research* **12** (2011) 2825-2830. <https://scikit-learn.org/stable/about.html> (Accessed 10 February 2025)

[27] A. Y-T. Wang, R. J. Murdock, S. K. Kauwe, A. O. Oliynyk, A. Gurlo, T. D. Sparks, *et al.* Machine Learning for Materials Scientists: An Introductory Guide toward Best Practices. *Chemistry of Materials* **32** (2020) 4954-4965.
<https://doi.org/10.1021/acs.chemmater.0c01907>

[28] T. Akiba, S. Sano, T. Yanase, T. Ohta and M. Koyama Optuna: A Next-generation Hyperparameter Optimization Framework. *ArXiv* (2019).
<https://doi.org/10.48550/arXiv.1907.1090>

[29] GitHub, Extract the most desirable functional groups/fragments for TDP1 inhibition, https://github.com/articlesmli/IUPAC_ML_model_TDP1/blob/main/IUPAC_ML_model/5.5.TDP1_group_all_dfs.ipynb (Accessed 17 July 2025)

[30] GitHub, Extract the least desirable functional groups/fragments for TDP1 inhibition, https://github.com/articlesmli/IUPAC_ML_model_TDP1/blob/main/IUPAC_ML_model/5.5.TDP1_group_all_dfs_ZEROS.ipynb (Accessed 17 July 2025)

[31] LibreTexts: Chemistry, Characteristics of ^{13}C NMR Spectroscopy, [https://chem.libretexts.org/Bookshelves/Organic_Chemistry/Organic_Chemistry_\(Morsch_et_al.\)/13%3A_Structure_Determination_-_Nuclear_Magnetic_Resonance_Spectroscopy/13.10%3A_Characteristics_of_C_NMR_Spectroscopy#:~:text=13C%20NMR-,Summary,understanding%20chemical%20properties%20and%20reactivities](https://chem.libretexts.org/Bookshelves/Organic_Chemistry/Organic_Chemistry_(Morsch_et_al.)/13%3A_Structure_Determination_-_Nuclear_Magnetic_Resonance_Spectroscopy/13.10%3A_Characteristics_of_C_NMR_Spectroscopy#:~:text=13C%20NMR-,Summary,understanding%20chemical%20properties%20and%20reactivities) (Accessed 17 July 2025)

[32] S. Kuhn, C. Cobas, A. Barba, S. Colreavy-Donnelly, F. Caraffini, R. Moreira Borges. Direct deduction of chemical class from NMR spectra, *Journal of Magnetic Resonance* 348 (2023)107381. <https://doi.org/10.1016/j.jmr.2023.107381>

[33] ACD/Labs. Home page. <https://www.acdlabs.com/solutions/nmr-spectroscopy/> (Accessed 17 July 2025)